Photoionization Efficiency Spectrum and Ionization Energy of OBrO

R. Peyton Thorn, Jr.*,† and Louis J. Stief*,‡

Laboratory for Extraterrestrial Physics, NASA/Goddard Space Flight Center, Greenbelt, Maryland 20771

Thomas J. Buckley§ and Russell D. Johnson, III||

Physical and Chemical Properties Division, National Institute of Standards and Technology, Gaithersberg, Maryland 20899

Paul S. Monks⊥

Chemistry Department, University of Leicester, Leicester, LEI 7RH, U.K.

R. Bruce Klemm*,¶

Brookhaven National Laboratory, Bldg. 815, P.O. Box 5000, Upton, New York 11973-5000

Received: May 11, 1999; In Final Form: August 5, 1999

The photoionization efficiency (PIE) spectrum of OBrO was measured over the wavelength range $\lambda = 86-126$ nm using a discharge flow-photoionization mass spectrometer (DF−PIMS) apparatus coupled to a VUV synchrotron radiation source. Bromine dioxide was generated in a flow tube reactor by first forming BrO via the reaction $O(^3P) + Br_2$ and then allowing the BrO to react on the cold flow tube wall. The PIE spectrum of the BrO reactant was obtained and the photoionization threshold evaluated from the half-rise point of the step at threshold. This remeasurement yields IE(BrO) = 10.48 ± 0.02 eV, which supersedes our previous result. The PIE spectrum of OBrO displayed steplike behavior near threshold. A value of 10.29 ± 0.03 eV was obtained for the adiabatic ionization energy (IE) of OBrO from analysis of the photoionization threshold at $\lambda = 120.5$ nm. An ab initio determination of the IE of OBrO using the CCSD(T)/6-311+G(3df)//CCD/6-311+G(3df) level of theory gives a value of 10.26 ± 0.06 eV, which is in excellent agreement with the experimental result. The results are compared with previous determinations of the IE for both halogen monoxides, XO, and halogen dioxides, OXO (X = Cl, Br, I).

Introduction

Halogen oxides play an important role in atmospheric chemistry, especially in catalytic reaction cycles involved in stratospheric ozone depletion. Of particular significance are the catalytic cycles involving ClO and BrO which couple chlorine and bromine chemistries via reaction 1:

$$ClO + BrO \rightarrow OClO + Br \quad (1a)$$

$$\rightarrow ClOO + Br \quad (1b)$$

$$\rightarrow BrCl + O_2 \quad (1c)$$

OClO has been detected in the stratosphere over Antarctica, and its presence is thought to be due to the occurrence of reaction 1a.[1] The chemical and spectroscopic properties of OClO have been well characterized in laboratory studies, but much less is known about the bromine analogue. Very recently, the possible role of OBrO in the atmosphere has been considered.[2] OBrO was tentatively detected in the stratosphere by Renard et al.[2a] and therefore it might be a temporary nighttime reservoir species. The possible detection of OBrO is based on the observation of several peaks in the UV/visible spectrum observed during nighttime balloon flights at middle and high latitudes combined with the authors' identification of these peaks with features due to OBrO. However, model calculations performed by Chipperfield et al.[2b] indicate much smaller stratospheric abundances for OBrO than those suggested by the measurements of Renard et al.[2a]

The first observation of gas-phase OBrO in the laboratory was reported by Butkovskaya et al.[3] using the discharge flow−mass spectrometry technique. Flow tube effluent was passed through a nozzle-skimmer to form a molecular beam, focused through an inhomogeneous magnetic field to select paramagnetic species such as Br and OBrO, and then subjected to mass spectrometric detection. They detected the paramagnetic OBrO molecule with a lifetime >10 s among the products of the reaction $O(^3P) + Br_2$ in a discharge flow system operated at room temperature and a total pressure of 4 Torr. Further experiments,[3] in which Br_2 was introduced at the upstream end of the flow tube (with a reaction time of about 0.1s), showed that the OBrO signal increased when the O-atom source was turned off. This observation was interpreted as evidence for the reaction of OBrO with $O(^3P)$ and for accumulation of OBrO on the wall of the flow tube. OBrO has also been observed by absorption spectroscopy in the bromine photosensitized decom-

* Authors to whom correspondence should be addressed.
† E-mail: robert.p.thorn@gsfc.nasa.gov.
‡ E-mail: louis.j.stief@gsfc.nasa.gov.
§ E-mail: thomas.buckley @nist.gov.
|| E-mail: russell.johnson @nist.gov.
⊥ E-mail: p.s.monks@le.ac.uk.
¶ E-mail: klemm@sun2.bnl.gov.

10.1021/jp991555n CCC: $18.00
Published on Web 09/30/1999

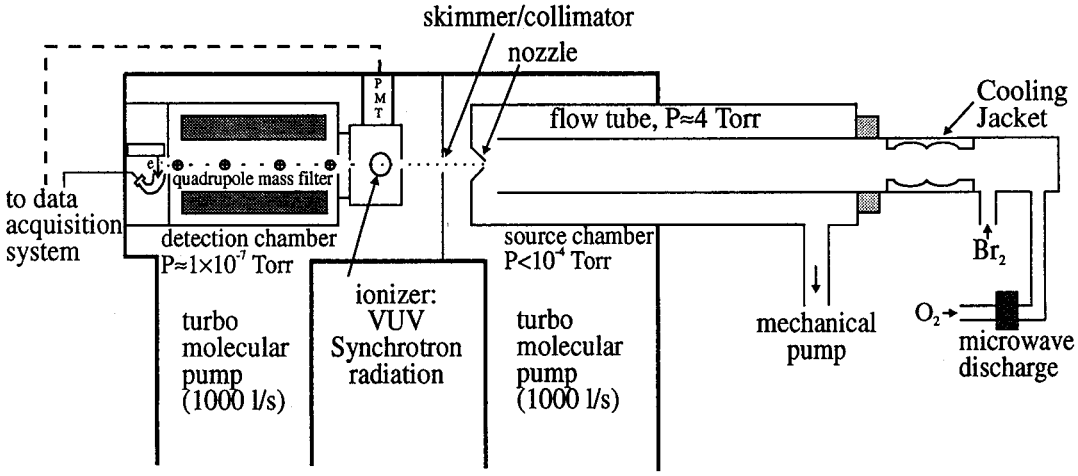

Figure 1. Schematic diagram of the DF−PIMS apparatus including the jacketed flow tube.

position of ozone by Rattigan et al.[4] and Rowley et al.[5] at $T =$ 298 K and up to one atmosphere total pressure. Rattigan et al.[4] also observed the same banded OBrO spectrum in the thermal reaction between Br_2 and O_3 at $T = 338$ K, after cessation of photolysis of $Br_2/O_3/O_2$ mixtures, and after pumping the gaseous mixture from the cell. The latter observation suggests that OBrO was efficiently absorbed on the cell wall and subsequently desorbed, consistent with the observations of Butkovskaya et al.[3] Müller et al.[6] and Miller et al.[7] showed that good yields of OBrO were obtained when the reaction products of an O_2/He discharge plus Br_2 were allowed to condense on the cell wall at $T = 250$ K. Signal due to OBrO was not observed while the gases were flowing, but strong OBrO signals were observed while pumping on the condensate that had collected on the cell wall. In contrast to these studies[6,7] which emphasize heterogeneous generation of OBrO, a very recent study by Li[8] attributed OBrO formation to only homogeneous processes.

Spectroscopic studies of OBrO have included measurements of the visible absorption spectrum,[4,5,7] the IR spectrum in the region of the ν_3 fundamental[6a] and the rotational spectrum in the submillimeter-wave region.[6] The visible spectrum has been identified as arising from the $C(^2A_2) \leftarrow X(^2B_1)$ electronic transition.[7] The OBrO rotational spectrum is that of a C_{2v}-symmetric molecule in the $^2B_1$ electronic ground state,[6] the same as for OClO. Butkovskaya et al.[3] had previously concluded that OBrO had C_{2v} symmetry based on their analysis of results obtained via focusing in an inhomogeneous electric field. The spectroscopic and thermodynamic properties of OBrO have been reviewed recently by Chase.[9] Pacios and Gomez [10a] and Francisco[10b] have reported ab initio calculations of properties such as equilibrium geometries,[10] vibrational frequencies,[10] and the adiabatic ionization energy[10b] of OBrO.

Following our previous photoionization mass spectrometric studies on halogen monoxides (FO,[11] ClO,[12] BrO,[13] IO[14]), hypohalous acids (HOCl,[15] HOBr,[16,17] HOI[18]) and dihalogen oxides (Cl_2O,[12] Br_2O[17]), we report here the first measurement of the photoionization efficiency (PIE) spectrum of OBrO. From the photoionization threshold of this spectrum, we obtain the first reported experimental determination of the ionization energy (IE) of OBrO. In addition, we present the results of an ab initio calculation of IE(OBrO) and compare the theoretical value with the experimental result.

Experimental Section

Experiments were performed by employing a discharge flow−photoionization mass spectrometry (DF−PIMS) apparatus coupled to the VUV beamline U-11 at the National Synchrotron Light source (NSLS) at Brookhaven National Laboratory. The apparatus and procedures have been described in previous publications. [11−20]

As discussed in the Introduction, previous laboratory studies[3−7] have demonstrated that OBrO may be generated either from bromine-sensitized decomposition of O_3[4] or from an unidentified bromine oxide condensate[3,5−7] on a cold surface ($T \approx 253$ K). In the present study, the condensate formed readily on the cold flow tube wall from gaseous BrO, which was a product of the $O(^3P) + Br_2$ reaction. Our ambient temperature flow reactor was modified to provide cooling in the region between the discharge section and the main flow tube (see Figure 1). The distance between the new cooling jacket section (about 20 cm in length) and the sampling nozzle at the end of the flow tube is about 100 cm. The flow tube was cooled to temperatures between ambient and −20 °C by circulating fluid refrigerant (ethanol/water, 50/50 by volume) from a low-temperature reservoir through the jacketed section. The flow velocity was typically 1550−1600 cm s $^{-1}$ and the flow tube pressure was maintained at about 3 Torr with helium carrier gas. About 5% of the O_2 was converted in the microwave discharge, so the $[O] \approx 5 \times 10^{12}$ atoms cm^{-3} while the $[Br_2]$ was always in large excess at $0.5-2.0 \times 10^{14}$ molecules cm^{-3}. The concentration of OBrO generated was estimated to be in the range of $10^{11}-10^{12}$ molecules cm^{-3}.

Species observed mass spectrometrically at an ionization energy of 12.4 eV ($\lambda = 100.0$ nm) were OBrO, HOBr, BrO, and Br_2O plus residual Br_2. A typical mass spectrum obtained with the jacketed flow tube section at $T \sim 253$ K, the Br_2 and O_2 flows turned on and the O-atom discharge turned on is shown in Figure 2a while the spectrum obtained with the Br_2 and O_2 flows turned off and the O-atom discharge turned off is shown in Figure 2b. The conditions used in Figure 2a are preferable for the present experiments for two reasons: (1) the OBrO signal is larger and (2) the Br_2O signal is significantly smaller and, in fact, barely detectable. The HOBr and BrO signals are comparable under the conditions employed in both Figure 2, both parts a and b. The HOBr probably arises from the interaction of Br_2O with residual water on the walls of the flow tube.[17] Signal from BrO at $m/z = 95$ and 97 is presumably due to the presence of BrO in experiments with the discharge on and to dissociative ionization of both OBrO and Br_2O with the discharge on or off. Further study of the BrO^+ formation process is underway with the objective of determining ΔH_f (OBrO) from the appearance energy of BrO^+ from OBrO. In several runs

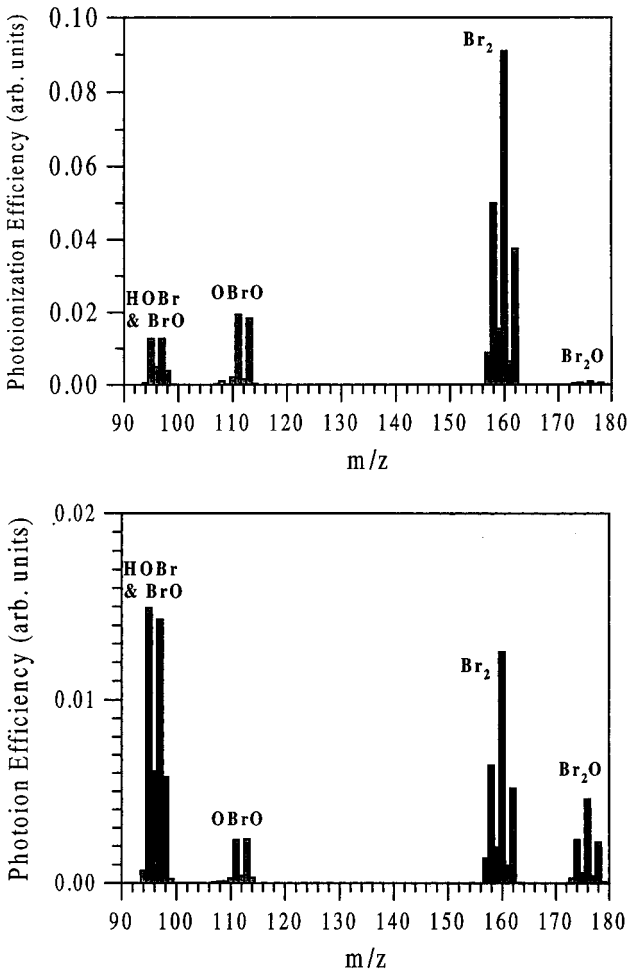

Figure 2. (a) Mass spectrum at $\lambda = 100.0$ nm (12.4 eV) with O_2 and Br_2 flows turned on and with the O-atom discharge turned on. Flow tube at $T = 253$ K (chilled section). Photoionization efficiency is ion counts divided by light intensity in arbitrary units. (b) Mass spectrum at $\lambda = 100.0$ nm (12.4 eV) with O_2 and Br_2 flows turned off and with the O-atom discharge turned off. Flow tube at $T = 253$ K (chilled section).

performed in the ambient temperature flow tube, mass spectra clearly displayed signal due to OBrO. However, the OBrO signal level in these runs was very low, only about 3% as large as for the low-temperature runs, and no further experiments were performed at ambient temperature.

The gaseous mixture in the flow reactor was sampled as a molecular beam into the source chamber and subsequently into the photoionization region of the mass spectrometer. Ions were mass selected with an axially aligned quadrupole mass filter, detected with a channeltron/pulse preamplifier, and counted for preset integration times. Measurements of PIE spectra (the ratio of ion counts/light intensity vs wavelength) were made using tunable vacuum-ultraviolet (VUV) radiation at the NSLS. A monochromator with a normal incidence grating (1200 lines/mm) was used to disperse the VUV light.[21] Since a LiF filter ($\lambda \geq 105$ nm) was not used, it was necessary to correct the PIE data for signal due to ionization by second-order light.[20,21] The intensity of the dispersed VUV light was monitored via a sodium salicylate coated window with an attached photomultiplier tube.

Helium (MG Industries, scientific grade, 99.9999%) and oxygen (MG Industries, 1.9% in scientific grade helium) were used as supplied. Bromine (Fluka, puriss.p.a. grade, >99%) was outgassed by repeated freeze−pump−thaw cycles.

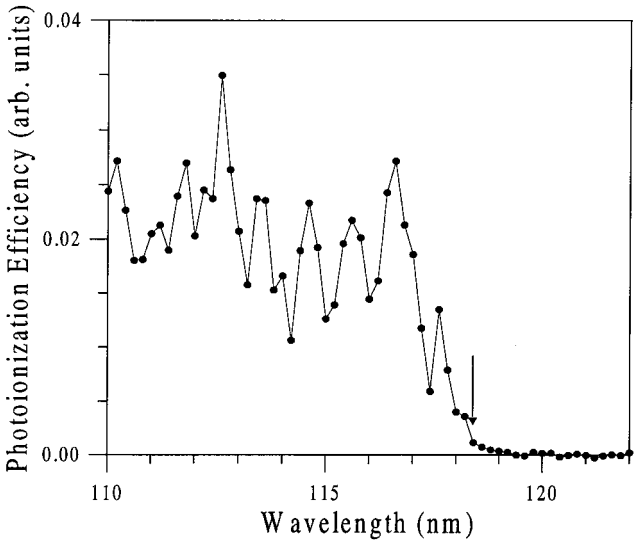

Figure 3. Photoionization efficiency spectrum of BrO ($m/z = 95$) between $\lambda = 110$ and 122 nm at a nominal resolution (fwhm) of 0.2 nm and with 0.2 nm steps. The arrow indicates the onset of ionization at $\lambda = 118.3_5$ nm (IE = $10.48_1 \pm 0.01_8$ eV). Flow tube at $T = 297$ K.

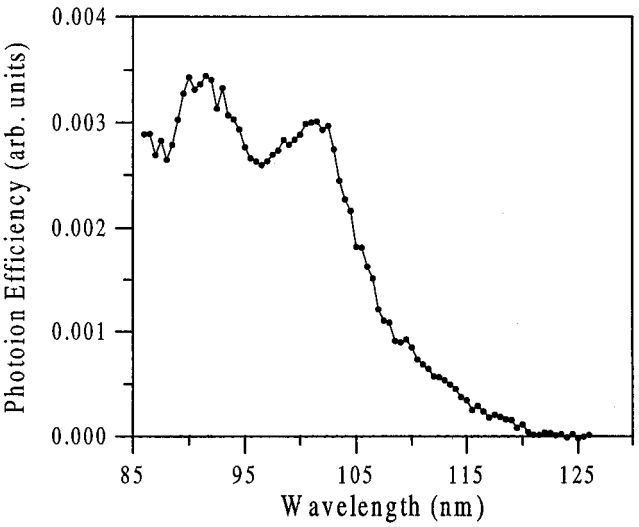

Figure 4. Photoionization efficiency spectrum of OBrO ($m/z = 113$) between $\lambda = 86$ and 126 nm at a nominal resolution (fwhm) of 0.2 nm and with 0.5 nm steps. Flow tube at $T = 254$ K (chilled section).

Results and Discussion

Since it was necessary to produce BrO in the flow tube as a first step in the generation of OBrO, PIE spectra were obtained to verify its formation. In Figure 3, we show the PIE spectrum for ^{79}BrO at $m/z = 95$ amu obtained over the wavelength range $\lambda = 110-122$ nm at a nominal resolution (fwhm) of 0.2 nm and with 0.2 nm steps. The photoionization threshold at $\lambda = 118.3_5$ nm was evaluated from the half-rise point of the step at threshold. This wavelength value corresponds to an ionization energy of $10.48_1 \pm 0.01_8$ eV. This remeasurement differs by only +0.02 eV from our earlier reported result[13] for IE(BrO), which was not evaluated from the half-rise point. This new result supersedes the older one.

The PIE spectrum for O^{81}BrO at $m/z = 113$ amu was obtained over the wavelength range $\lambda = 86-126$ nm and is shown in Figure 4. The nominal resolution (fwhm) is 0.2 nm and the step size is 0.5 nm. The peak signal-to-background ratio is more than 100:1. The spectrum displays some structure even at the moderate resolution employed. The structure shown by the O^{79}BrO spectrum at $m/z = 111$ amu is virtually identical.

TABLE 1: Ab Initio Calculations on Neutral and Cation OClO and OBrO

		OClO		$OClO^+$		OBrO		$OBrO^+$	
		expt[d]	calcd	expt[e]	calcd	expt[f]	calcd	expt	calcd
vibrational frequencies (cm^{-1})[a]	ν_1	945.6	870.6	1015 ± 40	996.4	795.7	756.2		842.8
	ν_2	447.7	408.6	520 ± 40	472.3	317	296		329.7
	ν_3	1110.1	1008		1238.1	848.6	793.6		912.9
	vzpe[h]	1251.7	1143.6		1353.4	980.7	922.9		1042.7
geometry[b]	r (Å)	1.473	1.4537		1.3892	1.649	1.6173		1.5654
	a (degrees)	117.60	116.9		121.4	114.4	113.3		115.2
energy (hartrees)[c]	energy		−609.787017		−609.410137		−2722.623607		−2722.248967
	energy with vzpe[h]		−609.781314		−609.403970		−2722.619139		−2722.244216
IE (eV)		10.33[e]	10.27				10.20		
final IE (eV)[g]							10.26		

[a] Calculated at BLYP/6-311+G(d). [b] Calculated at CCD/6-311+G(3df). [c] Calculated at CCSD(T)/6311+G(3df)//CCSD(T)/6311+G(3df). [d] Refs 26, 27. [e] Ref 25. [f] Refs 6,7. [g] The final IE was calculated using the reaction $OBrO + OClO^+ \rightarrow OBrO^+ + OClO$ (see text). [h] Vibrational zero-point energy.

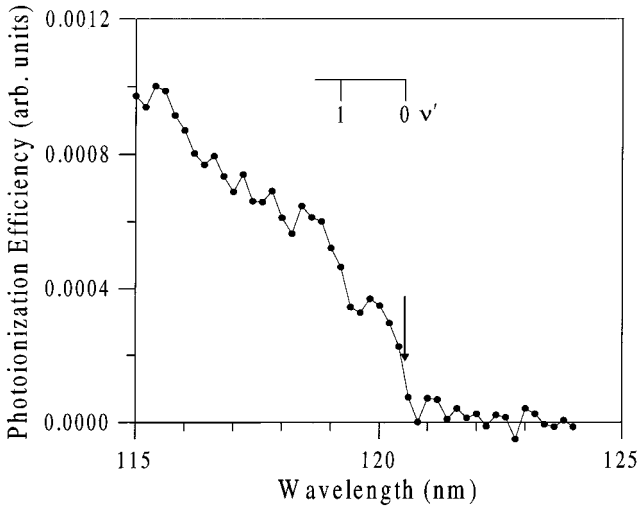

Figure 5. Photoionization threshold region of OBrO between $\lambda = 115$ and 124 nm at a nominal resolution (fwhm) of 0.2 nm and with 0.2 nm steps. This PIE spectrum is the sum of two independent experiments: one at $m/z = 113$ and one at $m/z = 111$. The arrow indicates the onset of ionization at $\lambda = 120.5_0$ nm (IE = 10.29 ± 0.03 eV). The superposed lines at 120.5 and 119.2 nm indicate the vibrational steps ($\nu' = 0,1$) in the OBrO cation. Flow tube at $T = 253-254$ K (chilled section).

To accurately determine the ionization energy, a series of spectra near the threshold were obtained and a detailed examination was carried out. Individual spectra of both $O^{79}BrO$ and $O^{81}BrO$ exhibited the same threshold to within ±0.1 nm. Therefore, PIE spectra with $m/z = 111$ and $m/z = 113$ were combined in a simple summation to produce the threshold scan, shown in Figure 5, over the wavelength region $\lambda = 115-124$ nm at a nominal resolution of 0.2 nm (fwhm) and with 0.2 nm steps. Each of the two independent experiments involved 6 or 7 wavelength scans. The spectrum displays the vibrational (symmetric stretch) steps ($\nu' = 0,1$) in the OBrO cation ground state with a spacing of 905 ± 98 cm^{-1}. The threshold, which appears to be a step function, was analyzed by determining the half-rise point as indicated in Figure 5. The threshold wavelength is 120.5 nm with an estimated uncertainty of ±0.3 nm. This uncertainty represents the sum of the instrumental resolution (±0.2 nm) and the precision in the threshold determination (±0.1 nm). From the threshold wavelength we obtain IE(OBrO) = 10.29 ± 0.03 eV.

We have also carried out ab initio calculations of the ionization energies of OBrO and OClO using the GAUSSIAN 94 series of programs.[22] Geometries were optimized at the MP2/6-311+G(d) level, and vibrational frequencies were computed. The vibrational frequencies for the cations are overly sensitive to the level of theory used. The cations are isovalent with ozone, a molecule with known computational difficulties.[23,24] We found that BLYP/6-311+G(3df) reproduced the vibrational frequencies of ozone, as well as the known vibrational frequencies of $OClO^+$. The zero-point vibrational energies were calculated using the experimental values for OClO and OBrO and the unscaled BLYP/6-311+G(3df) values for the cations. The geometry was refined at the CCD/6-311+G(3df) level, and final energies were computed at CCSD(T)/6-311+G(3df)//CCD/6-311+G(3df). The results are shown in Table 1 and compared with experimental values.[6,7,25−27] The vibrational frequency for the symmetric stretch (ν_1) is calculated to be 843 cm^{-1} compared to Francisco's value of 822 cm^{-1} calculated at a higher level of theory.[10b] Our experimental estimate of 905 ± 98 cm^{-1}, although not very precise, is consistent with both calculations. The geometric changes on ionization follow the generalizations by Walsh.[28] For a symmetric triatomic with 19 valence electrons, the lone electron occupies an orbital which is XO antibonding. On removal of the electron to form the OXO cation the XO bond length decreases. To overcome some of the systematic errors inherent in the calculations, the ionization energy of OBrO was determined by calculating the energy for the isogyric (same spin), homodesmic (similar bond types) reaction $OClO^+ + OBrO \rightarrow OClO + OBrO^+$. The energy for this reaction is −0.066 eV at the CCSD(T)/6-311+G(3df)//CCD/6-311+G(3df) level of theory. Using the experimental[25] IE(OClO) of 10.33 eV yields an IE(OBrO) of 10.26 eV. The estimate of the uncertainty, 0.06 eV, comes from the difference between the calculated IE (OClO) of 10.27 eV and the experimental value[25] of 10.33 eV. The calculated IE(OBrO) of 10.26 ± 0.06 eV is in excellent agreement with our measured value of 10.29 ± 0.03 eV. A recent calculation by Francisco[10b] employed a higher level of theory for the geometry and reports an uncorrected value of IE(OBrO) = 10.16 eV. The same reaction as above can be used with Francisco's calculated values to yield a corrected IE(OBrO) = 10.25 eV, which is very close to the above calculation and in excellent agreement with our experimental result. These methods would be expected to yield good results for other BrO_x species.

A comparison of the experimental ionization energies for the species XO and OXO (where X = Cl, Br, and I) is presented in Table 2. The value for IE(OIO) is a rough estimate based on trends observed in the values listed in the table. The ionization energy for both XO and OXO decreases for the series X = Cl → Br but much less so for OXO than for XO. If the trend continues for X = I, as suggested by the entry in the table for OIO, there should be a reversal in the trend between XO and OXO with IE(XO) > IE(OXO) for X = Cl and Br but IE(OXO) > IE(XO) for X = I.

TABLE 2: Ionization Energies for XO and OXO

XO species	XO IE/eV	OXO species	OXO IE/eV
ClO	10.88 ± 0.02[a]	OClO	10.33 ± 0.02[b]
BrO	10.48 ± 0.02[c]	OBrO	10.29 ± 0.03[c]
IO	9.74 ± 0.02[d]	OIO	$\sim 10.2 \pm 0.1$[e]

[a] Ref 12. [b] Ref 25. [c] This Study. [d] Ref 14. [e] Estimated from trend analysis.

Acknowledgment. The authors thank Dr. Charles Miller and Dr. Stanley Sander for helpful discussions and for providing details concerning the production of OBrO in a discharge flow system. R.P.T., Jr., thanks the NAS/NRC for an award of a Resident Research Associateship. The work at GSFC was supported by the NASA Upper Atmosphere Research Program. The work at BNL was supported by the NASA Upper Atmosphere Research Program and by the Chemical Sciences Division, Office of Basic Energy Sciences. U.S. Department of Energy, under Contract No. DE-AC02-76CH00016. Mention of manufacturers and brand names is to provide a complete description of the apparatus and does not imply endorsement by the National Institute of Standards and Technology or that the items are the best available for their purpose.

References and Notes

(1) (a) Solomon, S.; Mount, G. H.; Sanders, R. W.; Schmeltekopf, A. L. *J. Geophys. Res.* **1987**, *92*, 8329. (b) Solomon, S.; Sanders, R. W.; Miller, H. L., Jr. *J. Geophys. Res*. **1990**, *95*, 13807.

(2) (a) Renard, J.-B.; Lefevre, F.; Pirre, C.; Robert, C.; Huguenin, D. *C. R. Acad. Sci. Paris* **1997**, *325*, 921. Renard, J.-B.; Pirre, C.; Robert, C.; Huguenin, D. *J. Geophys. Res.* **1998**, *103*, 25383. (b) Chipperfield, M. P.; Glassup, T.; Pundt, I.; Rattigan, O. V. *Geophys. Res. Lett.* **1998**, *25*, 3575.

(3) Butkovskaya, N. I.; Morozov, I. I.; Tal′rose, V. L.; Vasiliev, E. S. *Chem. Phys.* **1983**, *79*, 21.

(4) Rattigan, O. V.; Jones, R. L.; Cox, R. A. *Chem. Phys. Lett.* **1994**, *230*, 121. Rattigan, O. V.; Cox, R. A.; Jones, R. L. *J. Chem. Soc., Faraday Trans.* **1995**, *91*, 4189.

(5) Rowley, D. M.; Harwood: M. H.; Freshwater, R. A.; Jones, R. L. *J. Phys. Chem.* **1996**, *100*, 3020.

(6) (a) Müller, H. S. P.; Miller, C. E.; Cohen, E. A. *Angew. Chem., Int. Ed. Engl.* **1996**, *35*, 2129. (b) Müller, H. S. P.; Miller, C. E.; Cohen, E. A. *J. Chem. Phys.* **1997**, *107*, 8292.

(7) Miller, C. E.; Nickolaisen, S. L.; Francisco, J. S.; Sander, S. P. *J. Chem. Phys.* **1997**, *107*, 2300.

(8) Li, Z. *J. Phys. Chem. A* **1999**, *103*, 1206.

(9) Chase, M. W. *J. Phys. Chem. Ref. Data* **1996**, *25*, 1069.

(10) (a) Pacios, L. F.; Gómez, P. C. *J. Phys. Chem. A* **1997**, *101*, 1767. (b) Francisco, J. S. *Chem. Phys. Lett.* **1998**, *283*, 307.

(11) Zhang, Z.; Kuo, S.-C.; Klemm, R. B.; Monks, P. S.; Stief, L. J. *Chem. Phys. Lett.* **1994**, *229*, 377.

(12) Thorn, R. P., Jr.; Stief, L. J.; Kuo. S.-C.; Klemm, R. B. *J. Phys. Chem.* **1996**, *100*, 14178.

(13) Monks, P. S.; Stief, L. J.; Krauss, M.; Kuo, S.-C.; Klemm, R. B. *Chem. Phys. Lett.* **1993**, *211*, 416.

(14) Zhang, Z.; Monks, P. S.; Liebman, J. F.; Huie, R. E.; Kuo, S.-C.; Klemm, R. B. *J. Phys. Chem.* **1996**, *100*, 63.

(15) Thorn, R. P., Jr.; Stief, L. J.; Kuo, S.-C.; Klemm, R. B. *J. Phys. Chem. A* **1999**, *103*, 812.

(16) Monks, P. S.; Stief, L. J.; Krauss, M.; Kuo, S.-C.; Klemm, R. B. *J. Chem. Phys*. **1994**, *100*, 1902.

(17) Thorn, R. P., Jr.; Monks, P. S.; Stief, L. J.; Kuo, S.-C.; Zhang, Z.; Klemm, R. B. *J. Phys. Chem.* **1996**, *100*, 12199.

(18) Monks, P. S.; Stief, L. J.; Tardy, D. C.; Liebman, J. F.; Zhang, Z.; Kuo, S.-C.; Klemm, R. B. *J. Phys. Chem.* **1995**, *99*, 16566.

(19) Tao, W.; Klemm, R. B.; Nesbitt, F. L.; Stief, L. J. *J. Phys. Chem.* **1992**, *96*, 104.

(20) Buckley, T. J.; Johnson, R. D., III; Huie, R. E.; Zhang, Z.; Kuo, S.-C.; Klemm, R. B. *J. Phys. Chem.* **1995**, *99*, 4879.

(21) Grover, J. R.; Walters, E. A.; Newman, J. K.; White, M. C. *J. Am. Chem. Soc*. **1985**, *107*, 7329.

(22) Frisch, M. J.; Trucks, G. W.; Schlegel, H. B.; Gill, P. M. W.; Johnson, B. G.; Robb, M. A.; Cheeseman, J. R.; Keith, T.; Petersson, G. A.; Montgomery, J. A.; Raghavachari, K.; Al-Laham, M. A.; Zakrzewski, V. G.; Ortiz, J. V.; Foresman, J. B.; Cioslowski, J.; Stefanov, B. B.; Nanayakkara, A.; Challacombe, M.; Peng, C. Y.; Ayala, P. Y.; Chen, W.; Wong, M. W.; Andres, J. L.; Replogle, E. S.; Gomperts, R.; Martin, R. L.; Fox, D. J.; Binkley, J. S.; Defrees, D. J.; Baker, J.; Stewart, J. P.; Head-Gordon, M.; Gonzalez, C.; Pople, J. A. *GAUSSIAN 94*, Revision E.2; Gaussian Inc.: Pittsburgh, PA, 1995.

(23) Li, X. Z.; Paldus, J. *J. Chem. Phys.* **1999**, *110*, 2844.

(24) Alcami, M.; Mo, O.; Yanez, M.; Cooper, I. L. *J. Phys. Chem. A* **1999**, *103*, 2793.

(25) Flesch, R.; Ruhl, E.; Hottmann, K.; Baumgartel, H. *J. Phys. Chem.* **1993**, *97*, 837. In addition to the PIMS result quoted, this study also reports a Photoelectron Spectroscopy (PES) result of IE(OClO) = 10.35 eV.

(26) Ortigoso, J.; Escribano, R.; Burkholder, J. B.; Lafferty, W. J. *J. Mol. Spectrosc*. **1992**, *155*, 25.

(27) Curl, R. F., Jr.; Kinsey, J. L.; Baker, J. G.; Baird, J. C.; Bird, G. R.; Heidelberg, R. F.; Sugden, T. M.; Jenkins, D. R.; Kenney, C. N. *Phys. Rev.* **1961**, *121*, 1119.

(28) Walsh, A. D. *J. Chem. Soc.* **1953**, 2266.